Strathprints Institutional Repository

Proceedings of Gas Turbine Technical Congress and Exposition
ASME Turbo Expo 2012
June 11-15, 2012, Copenhagen, Denmark

DRAFT GT2012-69223

ROBUST AERODYNAMIC DESIGN OF VARIABLE SPEED WIND TURBINE ROTORS

Edmondo Minisci
School of Engineering
James Watt Building South
University of Glasgow
University Avenue
Glasgow, G12 8QQ, UK
edmondo.minisci@glasgow.ac.uk

M. Sergio Campobasso*
School of Engineering
James Watt Building South
University of Glasgow
University Avenue
Glasgow, G12 8QQ, UK
sergio.campobasso@glasgow.ac.uk

Massimiliano Vasile
Department of Mechanical &
Aerospace Engineering
University of Strathclyde
75 Montrose Street
Glasgow, G1 1XJ, UK
massimiliano.vasile@strath.ac.uk

ABSTRACT

This study focuses on the robust aerodynamic design of the bladed rotor of small horizontal axis wind turbines. The optimization process also considers the effects of manufacturing and assembly tolerances on the yearly energy production. The aerodynamic performance of the rotors so designed has reduced sensitivity to manufacturing and assembly errors. The geometric uncertainty affecting the rotor shape is represented by normal distributions of the pitch angle of the blades, and the twist angle and chord of their airfoils. The aerodynamic module is a blade-element momentum theory code. Both Monte Carlo-based and the Univariate Reduced Quadrature technique, a novel deterministic uncertainty propagation method, are used. The performance of the two approaches is assessed both interms of accuracy and computational speed. The adopted optimization method is based on a hybrid multi-objective evolutionary strategy. The presented results highlight that the sensitivity of the yearly production to geometric uncertainties can be reduced by reducing the rotational speed and increasing the aerodynamic blade loads.

NOMENCLATURE

BM Root bending moment.
E_{BM} Mean of BM for given wind speed.
E_{TE} Mean of annual energy yield.
N_b Number of blades of the rotor.
R Tip radius.
TE Annual energy yield.
U Freestream wind velocity.
U_{rel} Relative wind velocity.
a Axial induction factor.
a' Circumferential induction factor.
r Radius along the blade.
$\mathbf{x}$ Array of design variables.
α Angle of attack.
θ_p Section pitch angle.
$\theta_{p,0}$ Blade pitch angle.
θ_T Blade twist angle.
λ Tip speed ratio.
σ Rotor solidity.
σ^2 Variance.
ϕ Angle of relative wind.
Ω Rotational speed.

INTRODUCTION

The present availability of large computational resources, and recent progress of design and optimization technologies offer the means to automate significant portions of product design. In the past few years, several studies on the use of diverse optimization techniques for the preliminary design of wind turbines have appeared. Some of these applications have focused on the optimization of existing blades by means of local search approaches, utilizing low- to medium-fidelity models. Due to the advances in global stochastic search methods, it has also been possible to

*Address all correspondence to this author.

work on design projects, in which no initial shape is considered and a global search is performed in a broad search space without the use of a starting point [1].

To accelerate the design process and achieve a sound design, two main factors must be considered: *a*) high-fidelity models should be introduced into the design process as early as possible, preferably since the preliminary design phase; *b*) the impact of shape and operational uncertainties on the performance should be assessed and minimized. The use of high-fidelity models and uncertainty quantification tools increases the computational cost of the design exercise, and this motivates the efforts aiming to develop new approaches allowing one to efficiently integrate high-fidelity and uncertainty propagation methods in the design system.

The uncertainty management and quantification requires the identification of suitable techniques, which can reliably predict and propagate uncertainty limiting the computational burden of the design task. The conceptually simplest way to propagate uncertainty through a general function is to sample the space of the independent variables by means of Monte Carlo (MC) methods [2]. Unfortunately, MC methods are computationally expensive, requiring a large number of function evaluations to converge. For this reason, researchers have been developing alternative, computationally more affordable approaches to uncertainty propagation. The main difficulty is to reduce computational costs with respect to MC methods while maintaining an acceptable accuracy of the probabilistic parameters of the output values. The techniques that have been proposed to accomplish these two conflicting requirements range from the Taylor-based method of moments [3, 4] to quadrature methods [5] and polynomial chaos expansion [6]. Among the proposed alternatives, an appealing one is the Univariate Reduced Quadrature (URQ) approach [7], which has been successfully used for the robust shape optimization of a transonic airfoil by means of a local gradient based search. The use of this deterministic sampling technique in robust design optimization based on global search methods is appealing and promising, but so far the URQ uncertainty propagation technique has not been used in global design optimization.

This paper focuses on the aerodynamic design of the bladed rotor of small horizontal axis wind turbines (HAWT's) with rated power of up to approximately 60 kW. More specifically, it analyzes the effects of manufacturing and assembly tolerances on the power and energy production of the turbine, and it includes such effects in the design optimization process. This procedure yields a robust aerodynamic design, namely a turbine rotor, the aerodynamic performance of which has minimal sensitivity to manufacturing and assembly errors. The main input parameters are the yearly wind distribution at the selected site, represented by a Weibull distribution, and the rotor swept area. The objective function is the yearly mechanical energy of the turbine. The geometric uncertainty affecting the rotor geometry is represented by normal distributions of the pitch angle of the blades, and the twist and chord of the airfoils making up the blades. The standard deviations associated with such distributions are representative of those observed in the manufacturing process of the turbine class considered in this paper. Moreover, since the rotor blades have the same nominal shape, two cases have been considered, namely one in which the stochastic shape of all blades is the same, and the other in which the stochastic shape of each blade varies independently from that of the other blades. The aerodynamic module is a blade-element momentum (BEM) theory code developed at the School of Engineering of Glasgow University.

Both the MC-based and the deterministic (URQ) uncertainty propagation methods have been tested to investigate how these sampling techniques behave when coupled with a global evolutionary search approach, and determine the best compromise between computational speed and accuracy for the level of standard deviations typical of this problem. The adopted optimization method is based on an evolutionary strategy (ES), which combines the exploratory capabilities of a multi-objective Estimation of Distibution algorithm [8, 9] with the exploitation capabilities of a differential evolution (DE)-based approach [10]. Given that the optimization is carried out taking into account the uncertainty of the design variables, the robust optimization consists of maximizing the mean of the yearly energy production and minimizing its standard deviation, leading to a multi-objective optimization problem.

The paper first describes the aerodynamic model, the main features of the two adopted optimizers and the strategy adopted for coupling all modules. The definition of the considered optimization problems is then provided, followed by a section presenting the validation of the selected methods of uncertainty propagation. This is followed by a section reporting the results of the robust design optimizations, and another presenting the comparative analysis of the turbine obtained without considering any geometry errors and one obtained by solving a robust design optimization problem. The concluding section summarizes the presented work and proposes further extensions of this study.

AERODYNAMIC MODEL

The aerodynamic module is WINSTRIP, a blade-element momentum (BEM) theory FORTRAN code [11]. This low-fidelity analysis tool is based on the radial subdivision of the rotor blades into sections or strips of radial width dr and mean radius r. For each strip, the flow data and the aerodynamic forces are determined by using two conditions. One condition is obtained by equating the thrust acting on the considered rotor ring determined by using the one-dimensional conservation of the linear momentum applied to the considered annular streamtube to that associated with the lift and drag forces acting on the segment (strip) of the blades intercepted by the annular streamtube. The other condition is obtained by equating the torque acting on the considered rotor ring determined by using the one-dimensional

conservation of the angular momentum applied to the considered annular streamtube to that produced by the lift and drag forces acting on the segment (strip) of the blades intercepted by the annular streamtube. The main geometric and aerodynamic parameters of a generic strip are depicted in Fig. 1, in which the sectional lift and drag forces are denoted by dF_L and dF_D respectively. Denoting by dT the thrust acting on a rotor ring, the elemental thrust coefficient is $dC_T = dT/(0.5\rho U^2 A)$, where R is the tip radius, $A = \pi R^2$ is the rotor surface, and ρ and U denote the freestream density and velocity respectively. The elemental thrust coefficient computed using the conservation of linear momentum is:

$$dC_T = 8a(1-a)\tilde{r}d\tilde{r} \tag{1}$$

where a is the axial induction factor, and the superscript $\tilde{}$ denotes nondimensionalization by R. The elemental thrust coefficient computed using lift and drag theory is:

$$dC_T = \frac{\sigma\lambda^2}{\cos^2\phi}(1+a')^2(C_L\cos\phi + C_D\sin\phi)\tilde{r}^2 d\tilde{r} \tag{2}$$

where $\sigma = (N_b c/(\pi R)$ is the rotor solidity, N_b is the number of blades of the rotor, c is the chord of the strip, $\lambda = \Omega R/U$, Ω is the angular speed of the rotor, a' is the circumferential induction factor and C_L, and C_D are the lift and drag coefficients respectively. The symbol ϕ denotes the angle of the relative wind velocity vector U_{rel} with respect to the rotor plane. Its expression is $\phi = \arctan[(1-a)/((1+a')\lambda\tilde{r})]$, whereas $U_{rel} = [(1-a)^2U^2 + (1+a')^2(\Omega r)^2]^{1/2}$. Equating expressions (1) amd (2) yields one equation in the two unknowns a and a'. This is because the coefficients C_L and C_D can be obtained from CFD codes or experimental data as functions of the Reynolds number, which depends linearly on U_{rel} and the relative angle of attack α, which is the angle between the airfoil chord and U_{rel}. As shown if Fig. 1, $\alpha = \phi - \theta_p$, where θ_p of the section pitch angle. This parameter depends only on geometric features, and its expression is $\theta_p = \theta_{p,0} + \theta_T$, where $\theta_{p,0}$ is the pitch angle of the blade and θ_T is the section twist angle. Denoting by dQ the torque acting on a rotor ring, the elemental torque coefficient is $dC_Q = dQ/(0.5\rho U^2 AR)$. The elemental torque coefficient computed using the conservation of angular momentum is:

$$dC_Q = 8a'(1-a)\lambda\tilde{r}^3 d\tilde{r} \tag{3}$$

The elemental torque coefficient computed using lift and drag theory is:

$$dQ_T = \frac{\sigma\lambda^2}{\cos^2\phi}(1+a')^2(C_L\sin\phi - C_D\cos\phi)\tilde{r}^3 d\tilde{r} \tag{4}$$

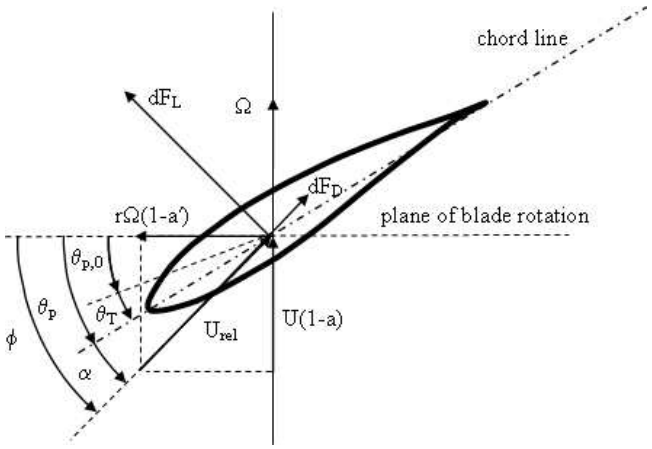

Figure 1. GEOMETRIC AND AERODYNAMIC PARAMETERS OF A GENERIC BLADE STRIP.

Equating expressions (3) amd (4) yields another equation in the two unknowns a and a'. The nonlinear system resulting by equating the two expressions of dC_T and dC_Q for each strip is solved with Newton's method. The C_L and C_D data are stored in tables as functions of the Reynolds number and α, and such data are computed in a pre-processing step using the MIT aerodynamic solver XFOIL. Tip and hub vortex losses are also included by means of the Prandtl tip loss model [11]. Once the flow state of each strip is known, the elemental power dP can be computed. WINSTRIP uses a nondimensional power coefficient $dC_P = dP/(0.5\rho U^3 A)$, the expression of which is:

$$dQ_T = \frac{\sigma\lambda^3}{\cos^2\phi}(1+a')^2(C_L\sin\phi - C_D\cos\phi)\tilde{r}^3 d\tilde{r} \tag{5}$$

The mechanical power corresponding to a particular value of U is determined by integrating Eqn. (5) from the blade root to its tip.

The set of input variables of the BEM code is made up of: U, Ω, N_b and the blade geometry. This latter is defined by root and tip radius, radial distributions of chord c and section twist θ_T, and blade pitch The set of output variables includes: mechanical power, rotor thrust, bending moment at the blade root, and radial distributions of all kinematic data (e.g. a, a', α) and aerodynamic forces. The WINSTRIP code has been validated by comparing its output with that of the National Renewable Energy BEM cosa WTPERF [12] using several realistic blade geometry. In all cases, the root-mean-square of the difference of all output radial distributions of kinematic and aerodynamic data is within machine error, which demonstrate the correctness of WINSTRIP.

HYBRID EVOLUTIONARY SOLVER

Evolutionary Algorithms (EA's) solve optimization problems by making a generation of individuals (turbines, in this study) evolve subject to selection and search operators. This iterative process eventually leads to a population containing the fittest possible individuals (best turbine designs), or individuals who are anyway significantly fitter than those of the starting population. The role of the selection operators is to identify the fittest or more promising individuals of the current population, whereas search operators such as crossover and mutation *attempt* to generate better offsprings starting from suitably selected individuals of the current generation. Each individual is defined by genes, which correspond to design variables in design optimization. The solution of the optimization problems reported in this study is based on a hybrid approach, which makes a combined use of two different EA's: the Multi-Objective Parzen-based Estimation of Distribution (MOPED) [8] and the Inflationary Differential Evolution Algorithm (IDEA) [10].

The MOPED algorithm belongs to a subset of EA's, and it was developed to circumvent certain algorithmic problems of conventional EA's. Standard EA's can be ineffective when the problem at hand features a high level of interaction among the design variables. This is mainly due to the fact that the recombination operators are likely to disrupt promising sub-structures that may lead to optimal solutions. Additionally, the use the crossover and mutatioan operators may result in slow convergence to the solution of the optimization, that is it may require a large number of generations to obtain very fit individuals. MOPED was developed to circumvent shortfalls of this kind. Its use of statistical tools enables it to preserve promising sub-structures associated with variable interaction from one generation to another (automatic linkage learning). Such statistical tools also replace the crossover and mutation operators of standard EA's, and they allow a faster convergence of MOPED with respect to the latter class of optimizers. Starting from the individuals of the current population, MOPED builds an approximate probabilistic model of the search space. The role of the crossover and mutation operators is replaced by sampling of this probabilistic model. There exist similar other evolutionary methods that use the aforementioned strategy, and they are called Estimation of Distribution Algorithms (EDA's) [13]. MOPED is a multi-objective optimization EDA for continuous problems that uses the Parzen method [14] to build a probabilistic representation of Pareto solutions, and can handle multivariate dependencies of the variables [8, 9]. This EDA optimizer implements the general layout and the selection techniques of the Non-dominated Sorting Genetic Algorithm II (NSGA-II) [15], but traditional crossover and mutation search approaches of NSGA-II are replaced by sampling of the Parzen model. NSGA-II was chosen as the base for MOPED mainly due to its simplicity, and also for the excellent results obtained for many diverse optimization problems using this approach [16, 17]

The Parzen method utilizes a non-parametric approach to kernel density estimation, and results in an estimator that converges everywhere to the true Probability Density Function (PDF). Additionally, when the true PDF is uniformly continuous, the Parzen estimator can also be made uniformly consistent. The Parzen method allocates N_{ind} identical kernels (where N_{ind} is the number of individuals of the current population), each one centered on a different element of the sample. Then,a probabilistic model of the promising search space portion is built on the basis of the statistical data provided by N_{ind} individuals through their kernels, and $\tau_E N_{ind}$ new individuals ($\tau_E \geq 1$) are sampled. The variance of each kernel depends on (i) the location of the individuals in the search space and (ii) the fitness value of these individuals, and its construction leads to values that favour sampling in the neighbourhood of the most promising solutions.

The features of MOPED often prevent the true Pareto front from being achieved, particularly when the front is broad and the individuals of the population are spread over different areas, which are far apart from each other in the feasible space. This circumstance has suggested to couple MOPED with another EA, which has better convergence properties. To this aim, the Inflationary Differential Evolution Algorithm (IDEA) [10] has been selected. IDEA was first developed for the design optimization of interplanetary trajectories, and it is an improved variant of the differential evolution (DE) algorithms [10]. The IDEA algorithm is based on a synergic hybridization of a standard DE algorithm and the strategy behind the monotonic basin hopping (MBH) [18]. The resulting algorithm was shown to outperform both standard DE optimizers and the MBH algorithm in the solution of challanging space trajectory design problems, featuring a multiple funnel-like structure. In this paper, a modified version of IDEA has been used to move the individuals of the approximate Pareto front obtained woth MOPED closer to the true front.

The main features of the original IDEA algorithm are reported in [10]. The IDEA algorithm works as follows: a DE process is performed several times and each process is stopped when the population contracts below a predefined threshold. At the end of each DE step, a local search is performed in order to get closer to the local optimum. In the case of non-trivial functions, there is a high likelihood of converging to local optima, the combined DE/local search is usually iterated several times, performing either a local or a global restart on the basis of a predefined scheduling.

The design optimization presented in this study is constrained. Therefore, the DE step must be modified so that the fitness assessment of the individuals during the DE process also take into account the constraints. The constraint handling technique used herein is one of the approaches that can be adopted in evolutionary computing, and is indeed the approach used by MOPED. In the unconstraint DE algorithm [19], and also in the unconstrained IDEA algorithm [10], each parent solution is compared with its offspring, and the solution with a better value of

the objective function is passed to the next generation. In the constrained case, on the other hand, when parents and offsprings are compared, the solutions are fist evaluated in terms of constraint compatibility cp. Its definition is: defined as:

$$cp(\boldsymbol{x}) = \sum_{j=1}^{m} s_j(\boldsymbol{x}) \tag{6}$$

where **x** is the array of design variables, m is the number of constraints, and the constraint factor d_j is:

$$s_j(\boldsymbol{x}) = \max\{g_j(\boldsymbol{x}), 0\} \tag{7}$$

The constraint factor equals 0 when the constraint is satisfied and is strictly positive when the constraint is violated. The solution with the better values of cp is then passed to the next generation. When the cp of parent and offspring are the same, the selection is performed based on the basis of the objective function.

In the current implementation, MOPED and IDEA are weakly coupled: the two algorithms are used one after the other. When MOPED reaches the maximum number of generations, clustered sub-populations of its final population are passed to IDEA as initial solutions. Since IDEA is a single objective optimizer, this algorithm moves the individuals of a sub-population of the MOPED front closer to the true Pareto front by considering a weighted sum of the original objective functions. The resulting hybrid optimizer blends the exploratory capabilities of MOPED (global exploration) and the favourable convergence characteristics of IDEA (exploitation of local information).

PROBLEM DEFINITION

In order to thoroughly analyze both the algorithmic and engineering aspects of the proposed robust design optimization system, the optimization problem has been formulated and solved in several different manners. On the algorithmic side, the aim of such analyses has been that of cross-comparing the computational cost of the MC and URQ methods for uncertainty propagation in the context of robust design optimization based on evolutionary methods, and also to assess strengths and weaknesses of both approaches in the context of global search methods. On the engineering side, two different definitions of the problem have been considered. One assumes that the shape of all the blades is identical, namely that identical manufacturing and assembly errors affect all blades of the rotor. The other assumes that such errors are not identical for all blades, though they are described by the same probability distribution functions. The latter scenario is representative of rotors the blades of which are manufactured and attached to the rotor separately. Therefore, 4 different optimization exercises have been performed, all with $N_b = 3$. The first optimization problem uses URQ sampling, assumes that the stochastic shape of all 3 blades is iiiidentical, and is denoted by URQ1; the second problem uses MC sampling, it also assumes that the stochastic shape of all 3 blades is iiiidentical, and is denoted by MC1;; the third problem, called URQ3, uses URQ sampling, but adopts a different set of geometric errors for each of the 3 blades of a given turbine; the fourth problem, MC3, also adopts a different set of geometric errors for each of the 3 blades of a given turbine, but it uses MC sampling for calculating the robust functionals.

In all 4 cases, The considered turbine type is regulated by rotational speed variations before the rated wind speed is reached, and is stall-regulated above the rated wind speed. The blades feature a single airfoil geometry, namely the NACA4413 airfoil, and the root and tip radii of the blades are fixed to $1.3[m]$ and $6.3[m]$ respectively. The nominal blade shape is parametrized by means of 6 design parameters defining the radial idstribution of the chord c, 6 design parameters defining the radial distribution of the twist angle θ_T, and 1 design parameter defining the blade pitch angle $\theta_{p,0}$. The rotational speed Ω associated with each wind speed is also a design variable. Since we considered 7 wind speeds, given by $U_i = 5 + i, \;\; i = 1,7$, we have 7 additional design variables, which are the 7 rotational speeds Ω_1 associated with the 6 wind speeds U_i. the total number of design parameters is thus 20. The rated wind speed of the considered turbine type typically varies between 10 and $12m/s$. Although power extraction also takes place beyond this range of rated speed, the analyses were limited to winds not exceeding 12 $[m/s]$. This was done because reliable airfoil force data were unavailable for the stalled regimes, and XFOIL cannot be used for stalled flows. This omission, however, is not believed to significantly affect the validity of the proposed robust design optimization technology for wind turbines, the presentation and application of which are impotant elements of this study. The design variables x_1 to x_6 are the chord c at the radial positions $(r_1 \;\; r_2 \;\; r_3 \;\; r_4 \;\; r_5 \;\; r_6) = (1.3 \;\; 2 \;\; 3 \;\; 4 \;\; 5 \;\; 6.3)[m]$, and the design variables x_7 to x_{12} are the twist θ_T at the same 6 radial positions. The shape of the blade is obtained by using the MATLAB® shape-preserving piecewise cubic interpolation function `pchip` over the 6 radial stations. The variable x_{13} is the blade pitch angle $\theta_{p,0}$, and the variables x_{14} to x_{20} are the 7 vallllues of Ω associated with the 7 considered values of U. The bounds of all design variables are given in Table 1.

The parameters to be set for the MOPED algorithm are: size of the population N_{ind}, number of constraint classes N_{cl}, fitness parameter α_f and sampling proportion τ_E. The values of these variables for the problem at hand are $N_{ind} = 100$, $N_{genMAX} = 100$, $N_{cl} = 3$; $\alpha_f = 0.5$; $\tau_E = 1$.

Since the adopted algorithms are designed to minimize objective functions, all 4 problems are set so as to have two objec-

x_1	$\in [0.10, 0.90]\ [m]$	$c(r_1)$
x_2	$\in [0.10, 0.90]\ [m]$	$c(r_2)$
x_3	$\in [0.10, 0.90]\ [m]$	$c(r_3)$
x_4	$\in [0.10, 0.60]\ [m]$	$c(r_4)$
x_5	$\in [0.10, 0.50]\ [m]$	$c(r_5)$
x_6	$\in [0.10, 0.40]\ [m]$	$c(r_6)$
x_7	$\in [0, 50]\ [deg]$	$\theta_T(r_1)$
x_8	$\in [0, 50]\ [deg]$	$\theta_T(r_2)$
x_9	$\in [0, 40]\ [deg]$	$\theta_T(r_3)$
x_{10}	$\in [0, 20]\ [deg]$	$\theta_T(r_1)$
x_{11}	$\in [0, 10]\ [deg]$	$\theta_T(r_5)$
x_{12}	$\in [0, 10]\ [deg]$	$\theta_T(r_6)$
x_{13}	$\in [-10, 10]\ [deg]$	$\theta_{p,0}$
x_{14-20}	$\in [50, 150]\ [rpm]$	$\Omega_i(U_i),\ \ i = 1, 7$

Table 1. RANGE OF DESIGN VARIABLES.

tives to minimize:

$$\begin{aligned} F_1 &= -E_{TE} \\ F_2 &= \sigma^2_{TE} \end{aligned} \tag{8}$$

where E_{TE} and σ^2_{TE} are respectively the mean value and the variance of the annual energy production TE in kWh. The considered constraints and the associated elements of constraint factors are respectively:

$$\begin{aligned} &C_1 : F_1 \leq -4e4 \\ &C_2 : F_2 \leq 2e7 \\ &C_3 : max(E_{BM}) \leq 12 \end{aligned} \tag{9}$$

$$\begin{aligned} &g_1 : (F_1 + 4e4)/4e4 \\ &g_2 : (F_2 - 2e7)/2e7 \\ &g_3 : (max(E_{BM}) - 12)/12 \end{aligned} \tag{10}$$

where the subscript BM denotes the bending moment ([kNm]) at the blade root, and the symbol E_{BM} denotes the expectation of BM for each of the 7 wind speeds.

The parameters defining the blade geometry are assumed to be affected by normally distributed uncertainty. These Gaussian distributions are centered at the nominal value of each parameter and have a standard deviation corresponding to $1cm$ for lengths and $\leq 2.5deg$ for angles. Since the optimizers use a nondimensionalized search space, with variables varying in the interval $\in [0,1]$, the vector of nondimensional standard deviations of each blade, obtained by dividing each standard deviation by the dimensional range of the corresponding variable, is $\boldsymbol{\sigma 1} = [0.0125\ \ 0.0125\ \ 0.0125\ \ 0.02\ \ 0.025\ \ 0.0333\ \ 0.05\ \ 0.05\ \ 0.05\ \ 0.1\ \ 0.2\ \ 0.2\ \ 0.1]$. In the URQ1 and MC1 cases, the 3 blades are taken to be identical and therefore the 13 geometric parameters define the whole rotor. As the deterministic sampling of URQ requires $2n+1$ evaluations [7], each robust analysis requires 27 computations of the full annual energy production, namely 189 runs of the BEM code. By contrast, 10000 samples (*i.e.* 70000 BEM runs) are performed in the MC1 case.

The implementation of problems URQ3 and MC3 is slightly more involved and its solution is computationally more expensive. The nominal geometry is still described by 13 parameters, but the sampling to statistically characterize objective functions and constraints is done considering that the geometric uncertainty affects each blade independently. Denoting $\boldsymbol{\mu 1}$ the vector of mean values for the case in which all three blades are identical, the mean and standard deviation vectors for the case in which each blade is affected by independent uncertainty are respectively $\boldsymbol{\mu 3} = [\boldsymbol{\mu 1}\ \ \boldsymbol{\mu 1}\ \ \boldsymbol{\mu 1}]^T$ and $\boldsymbol{\sigma 3} = [\boldsymbol{\sigma 1}\ \ \boldsymbol{\sigma 1}\ \ \boldsymbol{\sigma 1}]$. Each step of the URQ3 optimization requires $13x3x2+1 = 79$ evaluations of the annual energy production (483 BEM runs) whereas a sampling of 10000 individuals has been used for the MC3 case. In principle, each step of the MC3 optimization should have used a larger sampling base than the MC1 problem. This has not been done to maintain the overall cost of the MC3 analysis within affordable bounds and, as shown in the next section, the use of 10000 samples for each MC3 robust evaluation yields results with a sufficient level of convergence for optimization applications.

The parameters of the DE in IDEA are set as follows: weighting factor $F = 0.9$, crossover probability $CR = 0.9$, strategy "$DE/best/1/bin$". The IDEA algorithm stops when the population contracts to 25% of maximum expansion during the evolution [10].

The considered wind speeds and the corresponding relative cumulative times used to compute the annual energy production are depicted in Figure 2, This annual wind speed curve corresponds to a Weibull distribution with scale parameter $\lambda_W = 7$ and shape parameter $k = 2$.

In order to assess the impact of considering the manufacturing and assembly tolerances in the design optimization, a deterministic optimization, *i.e.* one not including and uncertainty, has also been carried out. The aforementioned assessment is then made by comparing the aerodynamic characteristic and the shape of the turbine obtained by using either the deterministic or the robust optimization approach. The deterministic optimization problem has a single-objective function, namely $F = -TE$,

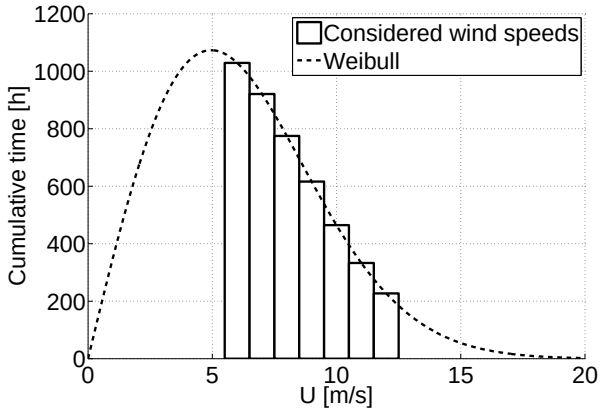

Figure 2. WIND SPEEDS AND CUMULATIVE TIMING USED TO COMPUTE THE ANNUAL ENERGY PRODUCTION.

and the constraints are:

$$\begin{aligned} C_1 &: F \leq -4e4 \\ C_2 &: max(BM) \leq 12 \end{aligned} \tag{11}$$

The process has been carried out using the IDEA optimizer, starting with a random population of 20 individuals.

ASSESSMENT OF SAMPLING TECHNIQUES

Before running the 4 optimizations, the URQ and MC sampling techniques have been assessed and compared both in terms of accuracy and computational requirements. Given a nominal blade geometry and the error distributions previously described, mean and standard deviation of TE and BM have been computed for 2 scenarios: a) all blades of the rotor are identical because identical manufacturing and assembly errors affect all blades, and b) the blades of the rotor are affected by different errors, though such errors belong to the same probability distribution function. The results of this analysis are summarized in Tables 2 and 3, which provide mean and variance values respectively. The symbol $\sigma^2_{maxE_{BM}}$ In the third column of Table 3 indicates the variance of the functional $maxE_{BM}$.

A good agreement between the URQ and MC results is observed. With either definition of the errors affecting the beometry of the blades, the mean of the annual energy computed with URQ and MC differs by less than 0.1%. The variance of this functional computed with URQ and MC differs at most by 5.3%. A good agreement between the URQ and MC approaches is also obtained for the bending moment: the difference of mean and variance values are at most 0.24% and 6.4% respectively. Note that using either definition of the geometric errors does not lead to differences of TE, but leads to differences of its variance. The variance of TE when the geometric errors are common to all 3 blades of a turbine is 3 times that obtained when the geometric errors of the 3 blades are different. The relationship between mean and variance using either definition of the geometry errors can also be obtained analytically by using the analytical expressions of the URQ mean and variance reported in [5].

Sampling technique	E_{TE} $[kWh]$	$max(E_{BM})$ $[kNm]$
URQ1	61136.9	5.2652
MC1	61191.7	5.2683
URQ3	61136.9	5.2652
MC3	61198.9	5.2693

Table 2. COMPARISON OF URQ AND MC SAMPLING TECHNIQUES: MEAN VALUES.

Sampling technique	σ^2_{TE} $[kWh^2]$	$\sigma^2_{maxE_{BM}}$ $[kNm^2]$
URQ1	26022484.6	0.3721
MC1	24922486.4	0.3498
URQ3	8674161.5	0.3721
MC3	8237023.3	0.3563

Table 3. COMPARISON OF URQ AND MC SAMPLING TECHNIQUES: VARIANCE VALUES.

Figures 3, and 4 show the convergence of the MC samplings, and their curves highlight that 10000 samplings are sufficient to obtain good convergence levels, which are adequate for evolutionary optimization processes.

RESULTS

Comparative analysis of robust optimizations

The hybrid optimizer is implemented in MATLAB® and, for the cases with MC sampling, it is also partially parallelized on a linux cluster, in order to accelerate the optimisation processes.

Based on 10000 robust function evaluations (100 nominal turbine geometries for each of the 100 populations), MOPED gives the estimation of the 4 Pareto fronts of problems URQ1, MC1, URQ3 and MC3 reported in Figures 5 and 6. Figure 5 reports the 2 clouds labeled URQ1 and MC1 corresponding to the final population determined by MOPED for problems URQ1 and MC1, along with two additional points labeled indURQ1 and indMC1, which are the solutions of the IDEA refinement for processes URQ1 and MC1, respectively. For both cases, the refinement process in performed as follows: given the final population of the MOPED process, a sub-population containing the solution maximizing the annual energy production is selected and used

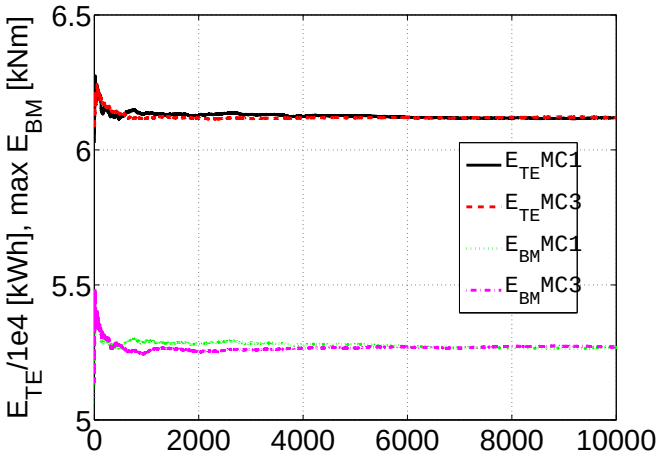

Figure 3. CONVERGENCE OF MC1 AND MC3 SAMPLINGS: MEAN VALUE OF ANNUAL ENERGY PRODUCTION AND ROOT BENDING MOMENT.

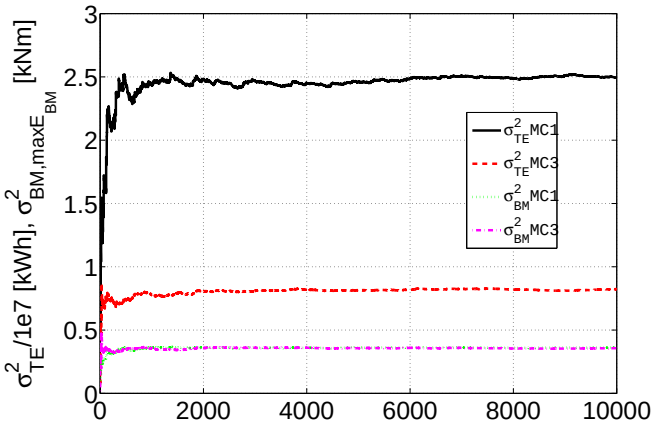

Figure 4. CONVERGENCE OF MC1 AND MC3 SAMPLINGS: VARIANCE OF ANNUAL ENERGY PRODUCTION AND ROOT BENDING MOMENT.

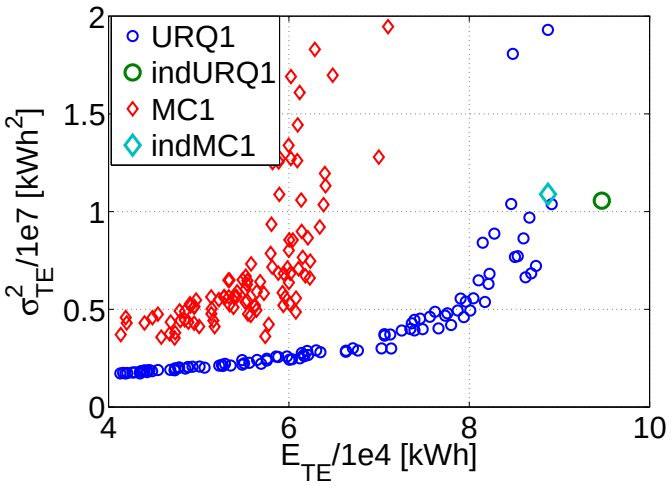

Figure 5. OPTIMIZATION RESULTS: PROBLEMS URQ1 AND MC1.

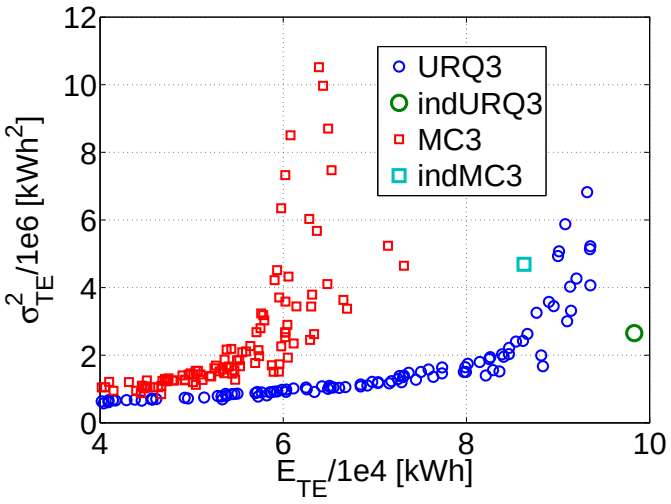

Figure 6. OPTIMIZATION RESULTS: PROBLEMS URQ3 AND MC3.

as stating point of the IDEA process. The aim of this latter is to maximize the annual energy production, subject to the constraints (9).

Figure 6 reports the solutions determined by MOPED for the problems URQ3 and MC3 along with two additional points labeled indURQ3 and indMC3, corresponding to solutions of the IDEA refinement for process URQ3 and MC3, respectively.

The comparison of the results obtained with URQ sampling (URQ1 and URQ3) and with MC sampling (MC1 and MC3) highlights that the sampling technique influences the convergence of the optimizers. More precisely, the two sampling approaches have different sensitivity to the irregularities of the BEM solver: when a nominal shape has in its neighborhood some blade geometries for which the BEM code does not converge, the MC approach has many more chances than the URQ approach to sample one or more of these ”defective” solutions; in this circumstance, since an undetermined solution cannot be used to compute the statistical characteristics of the performance, the nominal geometry itself is considered ”defective” and it is discarded (the corresponding solution vector is ranked poorly and, when compared to other solutions it has no chance to influence the rest of the evolution). When the URQ approach is used, the MOPED solver is able to quickly converge in regions of the search space corresponding to higher amounts of energy produc-

tion, while the high level of noise of the MC sampling slows down MOPED, which at the end of the allowed generations is still far from the pareto front.

The position of the refined IDEA solutions in the objective function space relative to the MOPED Pareto fronts helps to highlight the difficulties of having MOPED converge to the true Pareto front. The convergence of all multi-objective evolutionary algorithms to the true Pareto front of non trivial problems is always an asymptotic process [20], where the final results depend on the search capabilities (global exploration and local convergence) of the solver and the time (usually measured in generations) that the solver is allowed to run. If the solution of the problem is not *a priori* known, a measure of convergence can only be given by comparing the obtained solution to the best known one. As discussed in the section describing the MOPED and IDEA algorithms, IDEA has higher convergence capabilities and it stops only when contraction of the population below a certain threshold demonstrates the convergence to the optimum, which is a better approximation of a point of the Pareto front. Then, the distance between the Pareto approximation obtained by MOPED and the refinement obtained by IDEA gives a quality measure of the MOPED result. The solution indURQ1 (refinement of a sub-group of the final URQ1 population) is relatively close to the best solution obtained by the multi-objective solver, producing nearly 5500 kWh more, with unchanged variance (Figure 5). The better convergence properties of IDEA allow one to exploit the search space at the limit of the allowed constraint on the maximum bending moment. Almost the same happens for the refinement of an URQ3 sub-population, with solution indURQ3 producing nearly 4800 kWh more than the best solution (in terms of F_1) of the front, but in this case better performance in terms of energy production are also coupled to a reduction of the variance (Figure 6). Both refinement processes required a few hundred evaluations of the statistical characteristics: 1200 for indURQ1, and 1600 for indURQ3. In the MC1 case, the IDEA refinement leading to the indMC1 solution is actually able to greatly improve the performance obtained by MOPED, both reducing the variance of the solution and increasing the energy production by 17700 kWh, but it also required nearly 3600 evaluations of the statistical characteristics, just for the DE part of IDEA. The solution indMC1 tends to indURQ1, but the difficulties encountered by the MC sampling do not allow one to reach the same front. The comparison between optimization process adopting URQ3 and MC3 samplings highlight an analogous behaviour of the algorithms. The IDEA refinement pushes indMC3 solution toward the indURQ3 one, but due to the noise of the objective and constraint functions, and the initial difference of the starting points, indMC3 stops to a local optimum.

The differences between the indURQ1 and indMC1 solutions in terms of maximum power and annual energy as a function of the wind speed are shown in Figures 7 and 8 respectively. The statistical characteristics (mean and standard deviation) are evaluated by URQ sampling. The curves of Fig. 8 confirm what already shown in Fig. 5, namely that the refined solution indMC1 is as robust as the indURQ1 solution (the 2 standard deviations are similar), but provides lower nominal and mean annual energy. Note also that the energy peaks at 10 $[m/s]$ in Fig.8 are due to the fact that the product of power and number of hours at which this power level is achieved is maximum at this wind speed. The position of this maximum depends, other than the turbine characteristics, also on the wind distribution at the selected site. The top and bottom plots of Fig. 9 report the chord c and the pitch angle θ_pd radial profiles associated with the indURQ1, indMC1, indURQ3 and indMC3 solutions. The indMC1 nominal blade has twist angles that are higher than those of the indURQ1 nominal blade over most of the blade height. This leads to lower relative angles of attack and thus lift coefficients of the blade indMC1 over the blade indURQ1. Additionally, the $U-\Omega$ curve of the indMC1 turbine (not reported for brevity) is significantly lower than that associated with the turbine indURQ1. These 2 occurrences explain the lower energy production of the indMC1 turbine. On the other hand, the geometric differences between blades indURQ1 and indURQ3 are substantially smaller than those between blades indMC1 and indURQ1. The chord profiles obtained with the MC-based optimizations present minimal chord values in the root area, and structural loading issues make unlikely their practical use. On the other hand, the URQ blades have a smooth chord distribution. The pitch ngle profiles of the URQ blades are smooth but slightly unconvential. Nevertheless, it is expected that their shape would not pose any significant problem neither for structural integrity nor for manufacturing processes.

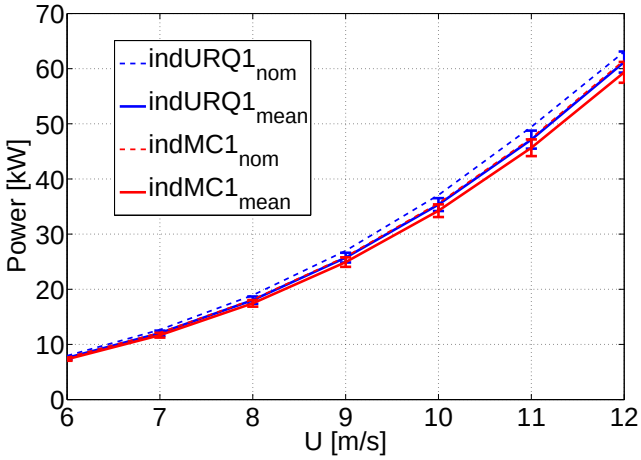

Figure 7. POWER CURVES FOR SOLUTIONS INDURQ1 AND INDMC1 (BOTH SOLUTIONS ARE EVALUATED BY URQ SAMPLING).

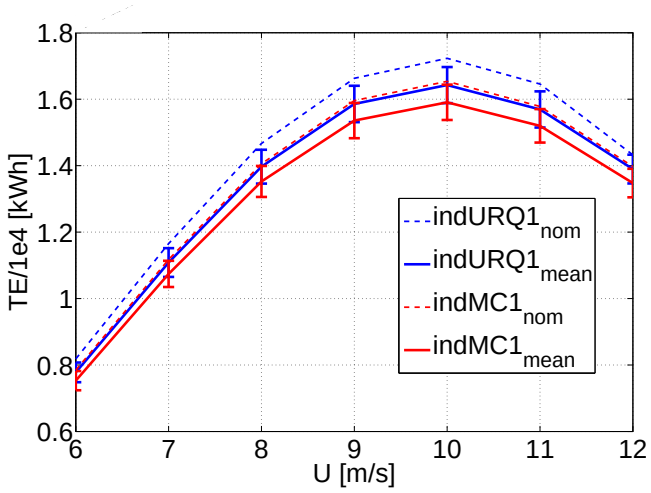

Figure 8. ANNUAL ENERGY YIELD: $INDURQ1_{NOM}$ AND $INDURQ1_{MEAN}$ ARE NOMINAL AND MEAN ENERGY YIELD OF SOLUTION INDURQ1; $INDMC1_{NOM}$ AND $INDMC1_{MEAN}$ ARE NOMINAL AND MEAN ENERGY YIELD OF SOLUTION INDMC1.

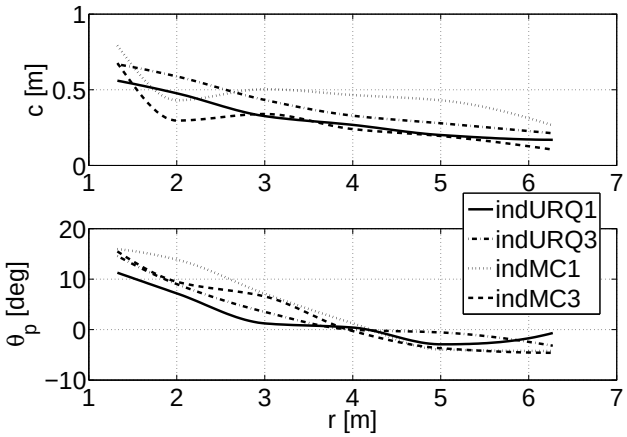

Figure 9. NOMINAL RADIAL PROFILES OF CHORD AND SECTION PITCH OF THE BLADES ASSOCIATED WITH SOLUTIONS INDURQ1, INDURQ3, INDMC1, and INDMC3.

The use of the MC sampling forces the optimizer to act in a conservative way with respect to the considered model. The stochastic properties of the solution of the problem inqMC1 evaluated by means of URQ sampling are very close to those obtained with the MC sampling. By contrast, the expectation and the variance of the inqURQ1 and indURQ3 solutions cannot be evaluated by means of the MC sampling. Making conservative analyses is often an important requirement in engineering applications. In this case, however, the conservative estimates of the MC-based optimization arise from the fact that the MC sampling suffers from an excessive sensitivity to irregularities of the BEM model, which do not necessarily correspond to actual characteristics of the real system. In other words, the fact that the BEM analysis of certain rotor geometries fails, does not necessarily imply that such configurations would deliver no power at all. The MC-based optimization, however, ignores completely such geometries, discarding significant portions of the design space presumably due to much smaller regions where the rotor geometry is truly unacceptable from an aerodynamic viewpoint.

Another important issue addressed by these analyses is the modeling decision as whether to assume in the uncertainty propagation process that all blades are affected by identical geometry errors or such errors randomly vary among the 3 blades. As discussed in the previous section, considering the same or different errors for all the blades appears not to affect the estimates of E_{TE}. Conversely, variance of the energy yoeld σ^2_{TE} is higher when considering identical geometry errors for all 3 blades. This implies that the robust design optimization based on this assumption is more pessimistic, and therefore, overly conservative, since the assumption of different manufacturing and assembly tolerances for the 3 blades is closer to reality. The effect of using either modeling of the geometry errors can be visualized by comparing the Pareto fronts reported in Fig. 5 and 5. The range of E_{TE} associated with the Pareto front of URQ1 and URQ3 are about the same, but the range of σ^2_{TE} of the URQ1 front is larger than that of the URQ3 front. Indeed, the constraint on σ^2_{TE} is active in the former case.

It should be noted that in the absence of active constraints, despite the fact that the Pareto fronts corresponding to either error model would have the same range of E_{TE} and a different range of σ^2_{TE}, the turbine geometries correspondingerror to a point of either front having the same E_{TE} would be the same. This is because the two two-objective optimizations would have a common objective function (E_{TE}) and would have the other objective function σ^2_{TE} which in one case is three times that of the other. Such a scaling would not affect the set of design variables corresponding to a solution of eother problem having the same E_{TE}. On the other hand, the presence of active constraints would break this correspondence, and therefore the use of either error model would lead to different turbine geometries giving the same E_{TE} This highlights the importance of selecting the most realistic model to account for the effects of manudacturing and assembly tolerances.

Comparative analysis of robust and deterministic optimizations

The optimal shape obtained by using the determinisitc optimization problem yields a nominal annual energy production of 100200 $[kWh]$, with expectation $E_{TE} = 93600$ $[kWh]$. Here this turbine, called indDET1, is compared to that associated with the indURQ1 solution, which has a nominal annual energy production of 99400$[kWh]$ and $E_{TE} = 94700$ $[kWh]$. As expected the

variance of the indDET1 turbine $\sigma^2_{TE} = 2.95e7\ \ [kWh^2]$ (computed with the URQ1 approach) is significantly higher than the indURQ1 turbine $\sigma^2_{TE} = 1.06e7\ \ [kWh^2]$. These numbers imply that the standard deviation of TE of the turbine indURQ1 is more than 40 % lower than that of the turbine indDET1.

The performance of the 2 turbines is compared in greater detail in Figures 10 and 11, which provide respectively the power and the annual energy of the 2 configurations. Here, $indURQ1_{nom}$ and $indURQ1_{mean}$ denote respectively nominal and mean values of the turbine indURQ1, while $indDET1_{nom}$ and $indDET1_{mean}$ denote nominal and mean values for the turbine indDET1. The statistical characteristics are evaluated by means of the URQ1 sampling. As expected, the indDET1 turbine has a slightly better nominal performance, but slightly worse mean values. More importantly, however, the power and annual energy variaces of the turbine indDet1 are significantly higher than those associated with the turbine indURQ1. This confirms that the use of robust design optimization yields turbine rotors which outperform, in a statistical sense, those obtained by using the deterministic design approach, which neglects the geometric errors associated with manufacturing and assembly tolerances.

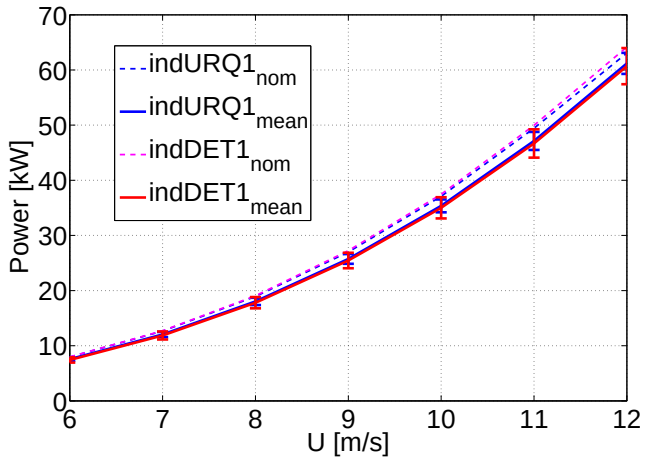

Figure 10. COMPARISON OF ROBUST AND DETERMINISTIC DESIGN: POWER CURVES.

The radial profiles of the chord c and the pitch angle θ_p of the 2 turbines are reported in the top and bottom plots of Fig. 12. One sees that chords of the 2 turbines are very close, whereas the picth angle distributions differ by up to about 3 *deg*. The optimal rotational speed of the 2 turbines for all considered wind speeds is reported in Fig. 13, which highlights that the turbine indURQ1 has lower Ω's than the turbine indDET1. The slope discontinuity of the curve indDET1 at $U = 11\ \ [m/s]$ is due to the fact that the constraint on the bending moment becomes active at $U = 12\ \ [m/s]$, reducing the rotational speed with respect to the case in which this constraint had remained inactive. To provide one more element to the comparative analysis of the 2 designs, the nominal and stochastic performance of the indDET1 rotor geometry using the rotational speeds of the indURQ1 geometry have been computed. The nominal and mean annual energy of this hybrid turbine configuration are 94600 $[kWh]$ and $E_{TE} = 91000\ \ [kWh]$ respectively. More importantly, however, the σ^2_{TE} value of the hybrid turbine is $2.95e7\ \ [kWh^2]$ is substantially higher that the value associated with the turbine indDET1. The performance of this hybrid configuration is poorer than that of both the indDET1 and indURQ1 configurations, as expected. The main conclusion of these analyses appears to be that design robustness (*i.e.* minimal variations of the annual energy yield due to manufacturing and assembly tolerances) can be achieved by adopting lower rotational speeds and compensating the reduction of power due to lower circumferential velocities by shifting upwards the radial profile of the lift coefficient. In turn, this can be achieved by increasing the angle of attack. This is the reason why the indURQ1 blade has lower values of θ_p: lower values of the pitch angle lead to higher values of α. An additional contribution to the increment of α also comes from the reduced circumferential speed, which results in higher values of the relative wind angle ϕ. The radial profile of the mean value of α along the blade for $U = 12\ \ m/s$ is reported in Figures 14, which confirms that the angle of attack along the indURQ1 blade is higher than that of the indDET1 blade due to the 2 effects highlighted above. Note also that the standard deviation of α for a given radial position is about the same for the 2 turbines. This is due to the fact that equal errors of the section pitch angle lead to equal variations of α. The higher values of the mean radial profile of α of the indURQ1 blade result in significantly higher values of the mean

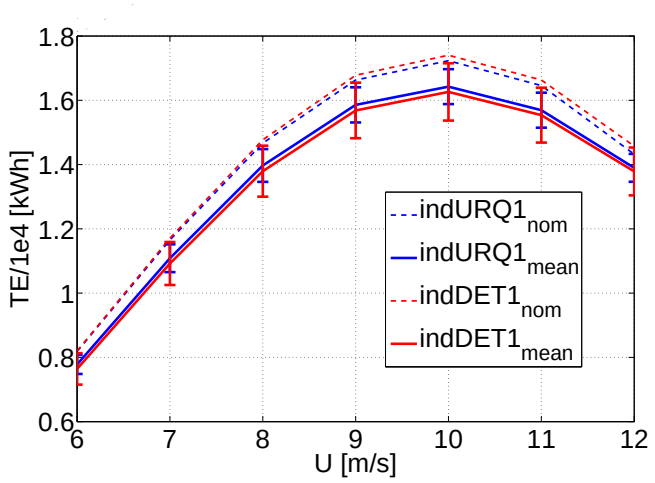

Figure 11. COMPARISON OF ROBUST AND DETERMINISTIC DESIGN: ANNUAL ENERGY YIELD.

profile of the lift coefficient C_L, as shown in Fig. 15, which also refers to $U = 12\ \ m/s$. It is important to note that the standard deviation of C_L of the blade indURQ1 is lower than that of the blade indDET1 along the entire blade height. This is because the levels of α along the outboard part of the indURQ1 blade are in a region where the slope of the $\alpha - C_L$ curve starts to decrease with respect to the linear part corresponding to lower angles of attack. Hence the variation of the lift coefficient caused by a given variation of α is smaller for the indURQ1 blade. The lower values of the standard deviation of C_L are the main reason for the lower standard deviation of the annual energy production of the turbine indURQ1 with respect to that of the turbine indDET1.

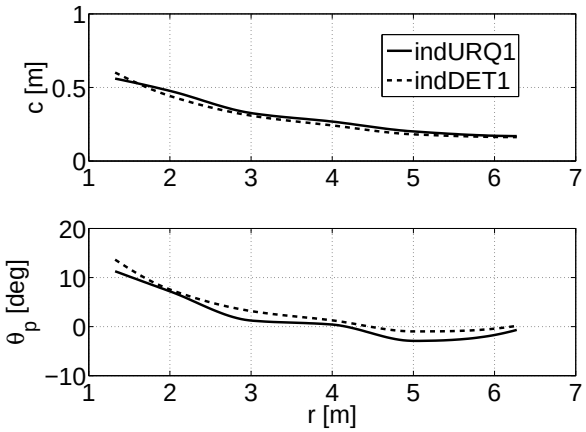

Figure 12. NOMINAL RADIAL PROFILES OF CHORD OF THE BLADES ASSOCIATED WITH SOLUTIONS INDURQ1, AND INDDET1.

CONCLUSIONS

A hybrid evolutionary algorithm has been applied to the robust design of a wind turbine rotor to maximise its annual energy production and minimize the variations of this parameter due to manufacturing and assembly tolerances of the blades. The uncertainty propagation based on MC sampling has been compared to the propagation based on the faster deterministic URQ sampling. The URQ approach better filters irregularities of the design space due to possible modeling limitations of the BEM model, and this feature, along with its high computational speed makes it an ideal tool for robust design optimization based on evolutionary algorithms.

The considered robust design optimization of a wind turbine rotor leads to a Pareto front of mean and standard deviation of annual energy yield. The comparative analysis of the turbine design obtained without the inclusion of any uncertainty, and the turbine design obtained considering manufacturing and assembly tolerances and having the same mean annual energy production of the deterministic optimum highlights that the standard deviation of the energy production of the robust optimal turbine design is more than 40 % lower than the value of this variable associated with the deterministically optimal turbine. The lower sensitivity to geometry errors is achieved by adopting lower rotational speeds and increasing the loading of the outboard part of the blade, moving to the range of higher values of the angle of attack where the slope of the $\alpha - C_L$ cirve is lower than for lower values of α.

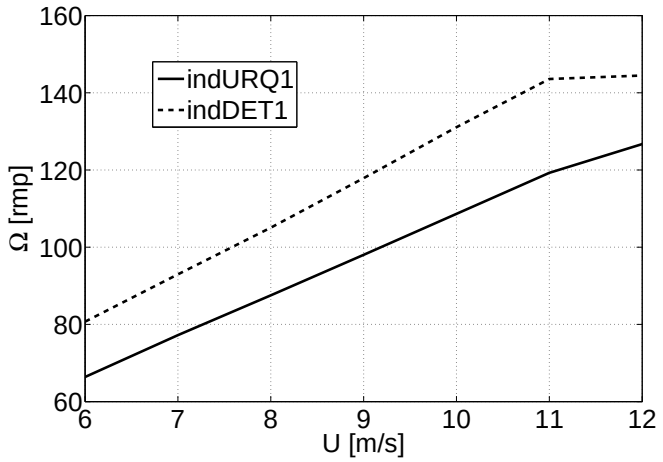

Figure 13. COMPARISON OF ROBUST AND DETERMINISTIC DESIGN: OPTIMAL ROTATIONAL SPEEDS ASSOCIATED WITH CONSIDERED WIND SPEED.

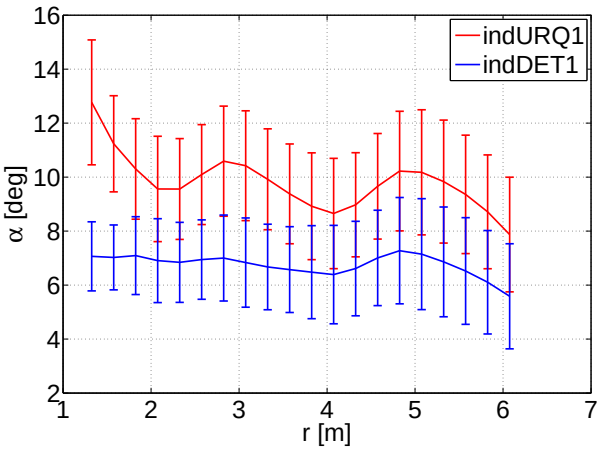

Figure 14. COMPARISON OF ROBUST AND DETERMINSITIC DESIGN: DISTRIBUTION OF α.

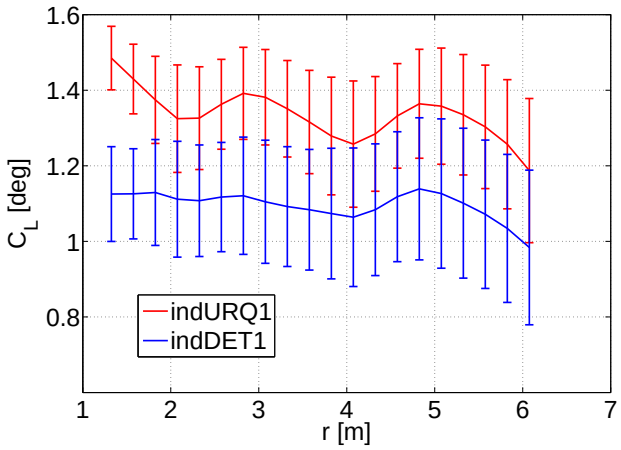

Figure 15. COMPARISON OF ROBUST AND DETERMINISTIC DESIGN: DISTRIBUTION OF C_L.

REFERENCES

[1] Benini, E., and Toffolo, A., 2002. "Optimal design of horizontal-axis wind turbines using blade-element theory and evolutionary computation". *Journal of Solar Energy Engineering*, ***124***, pp. 357–363.

[2] Helton, J., and Davis, F., 2003. "Latin hypercube sampling and the propagation of uncertainty in analyses of complex systems". *Reliability Eng. System Safety*, ***81***(1), pp. 23–69.

[3] Helton, J., and Davis, F., 2002. "Efficient uncertainty analysis methods for multidisciplinary robust design". *AIAA Journal*, ***40***(3), pp. 545–552.

[4] Putko, M., Newman, P., Taylor, A., and Green, L., 2001. "Approach for uncertainty propagation and robust design in cfd using sensitivity derivatives". In Proceedings of the 15th AIAA Computational Fluid Dynamics Conference, AIAA-20012528.

[5] Padulo, M., Campobasso, M., and Guenov, M., 2001. "Comparative analysis of uncertainty propagation methods for robust engineering design". In International Conference on Engineering Design ICED07.

[6] Xiu, D., and Karniadakis, E., 2003. "Modeling uncertainty in flow simulations via generalized polynomial chaos". *Journal of Computational Physics*, ***187***, pp. 137–167.

[7] Padulo, M., Campobasso, M., and Guenov, M., 2011. "A novel uncertainty propagation method for robust aerodynamic design". *AIAA Journal*, ***49***(3), pp. 530–543.

[8] Costa, M., and Minisci, E., 2003. "Moped: a multi-objective parzen-based estimation of distribution algorithm". In EMO 2003, Springer, pp. 282–294.

[9] Avanzini, G., Biamonti, D., and Minisci, E., 2003. "Minimum-fuel/minimum-time maneuvers of formation flying satellites". In Adv. Astronaut. Sci., pp. 2403–2422.

[10] Vasile, M., Minisci, E., and Locatelli, M., 2011. "An inflationary differential evolution algorithm for space trajectory optimization". *Evolutionary Computation, IEEE Transactions on*, ***15***(2), pp. 267–281.

[11] Manwell, J., McGowan, J., and Rogers, A., 2002. *Wind Energy Explained. Theory, Design and Application*. John Wiley and Sons Ltd.

[12] Buhl, M., 2011. WTPERF: a wind-turbine performance predictor, February. http://wind.nrel.gov/designcodes/ simulators/wtperf.

[13] , 2006. *Towards a New Evolutionary Computation: Advances on Estimation of Distribution Algorithms (Studies in Fuzziness and Soft Computing)*. Springer, February.

[14] Fukunaga, K., 1972. *Introduction to statistical pattern recognition*. Academic Press.

[15] Deb, K., Pratap, A., Agarwal, S., and Meyarivan, T., 2002. "A Fast and Elitist Multiobjective Genetic Algorithm: NSGA-II". *Evolutionary Computation, IEEE Transactions on*, ***6***(2), pp. 182–197.

[16] Datta, D., Deb, K., Fonseca, C., Lobo, F., Condado, P., and Seixas, J., 2007. "Multi-objective evolutionary algorithm for land-use management problem". *International Journal of Computational Intelligence Research*, ***3***(4), pp. 371–384.

[17] Deb, K., 2008. "Scope of stationary multi-objective evolutionary optimization: A case study on a hydro-thermal power dispatch problem". *Journal of Global Optimization*, ***41***(4), pp. 479–515.

[18] Leary, R., 2000. "Global optimization on funneling landscapes". *Journal of Global Optimization*, ***18***(4), pp. 367–383.

[19] Price, K., Storn, R., and Lampinen, J., 2005. *Differential Evolution: A Practical Approach to Global Optimization*. Springer.

[20] Deb, K., 2001. *Multi-Objective Optimization using Evolutionary Algorithms*. John Wiley and Sons Ltd.